Genetic Control of X Chromosome Inactivation in Mice: Definition of the *Xce* Candidate Interval

Lisa Helbling Chadwick,*,† Lisa M. Pertz,* Karl W. Broman,‡ Marisa S. Bartolomei§ and Huntington F. Willard*,1

Institute for Genome Sciences and Policy, Duke University, Durham, North Carolina 27708, †Department of Genetics, Case Western Reserve University, Cleveland, Ohio 44106, ‡Department of Biostatistics, Johns Hopkins University, Baltimore, Maryland 21205 and §Department of Cell and Developmental Biology, University of Pennsylvania School of Medicine, Philadelphia, Pennsylvania 19104

ABSTRACT

In early mammalian development, one of the two X chromosomes is silenced in each female cell as a result of X chromosome inactivation, the mammalian dosage compensation mechanism. In the mouse epiblast, the choice of which chromosome is inactivated is essentially random, but can be biased by alleles at the X-linked *X controlling element* (*Xce*). Although this locus was first described nearly four decades ago, the identity and precise genomic localization of *Xce* remains elusive. Within the X inactivation center region of the X chromosome, previous linkage disequilibrium studies comparing strains of known *Xce* genotypes have suggested that *Xce* is physically distinct from *Xist*, although this has not yet been established by genetic mapping or progeny testing. In this report, we used quantitative trait locus (QTL) mapping strategies to define the minimal *Xce* candidate interval. Subsequent analysis of recombinant chromosomes allowed for the establishment of a maximum 1.85-Mb candidate region for the *Xce* locus. Finally, we use QTL approaches in an effort to identify additional modifiers of the X chromosome choice, as we have previously demonstrated that choice in *Xce* heterozygous females is significantly influenced by genetic variation present on autosomes (CHADWICK and WILLARD 2005). We did not identify any autosomal loci with significant associations and thus show conclusively that *Xce* is the only major locus to influence X inactivation patterns in the crosses analyzed. This study provides a foundation for future analyses into the genetic control of X chromosome inactivation and defines a 1.85-Mb interval encompassing all the major elements of the *Xce* locus.

I N mammals, X chromosome inactivation serves to equalize X-linked gene expression between the sexes. Early in female development, each somatic cell inactivates one of its two X chromosomes. This choice is then faithfully transmitted to all daughter cells through mitosis, such that the adult female is a mosaic of two different cell lineages (LYON 1961). Two forms of X inactivation that differ in their mechanism of choice take place in the mouse embryo. The extraembryonic tissues undergo imprinted X inactivation, where the choice is dictated by parental origin. This results in nonrandom inactivation of the paternally inherited chromosome (TAKAGI and SASAKI 1975; HUYNH and LEE 2001; SADO et al. 2001; WANG et al. 2001; SADO and FERGUSON-SMITH 2005). In contrast, embryonic cells undergo random inactivation, and either X chromosome can be chosen for silencing (LYON 1961; KRIETSCH et al. 1986).

Although theoretically the two X chromosomes in a somatic cell have an equal chance of being inactivated, the X-linked locus *Xce* (**X** *controlling element*) can signif-

icantly bias this choice in mice (CATTANACH and ISAACSON 1967; CATTANACH and WILLIAMS 1972). Previous experiments have shown that *Xce* exerts a primary effect on choice, as skewed X inactivation patterns are observed even in embryos isolated soon after X inactivation occurs (RASTAN 1982) and because the effect persists even in the face of a selective advantage for one chromosome over the other (DREWS et al. 1974). Three alleles of *Xce* have been defined in inbred mouse strains on the basis of their influence on the X inactivation pattern in genetic crosses: a weak allele *Xceᵃ* (C3H/HeJ, 101/H, A/J, CBA/J and BALB/cByJ), an intermediate allele *Xceᵇ* (C57BL/6J, DBA/2J and JU/Ct), and a strong allele *Xceᶜ* (CAST/Ei), although additional alleles are thought to exist in other strains (CATTANACH et al. 1969; WEST and CHAPMAN 1978; JOHNSTON and CATTANACH 1981; SIMMLER et al. 1993). In *Xce* heterozygotes, the chromosome carrying the weaker of the two alleles is more likely to be inactivated. The degree of skewing can be quite profound; in *Xceᵃ/Xceᶜ* heterozygotes, the mean X inactivation pattern is ∼25:75, whereby the chromosome carrying the *Xceᵃ* allele is active in only one-quarter of cells (PLENGE et al. 2000; DE LA CASA-ESPERON et al. 2002). In contrast, choice in *Xce* homozygotes is largely unbiased (KRIETSCH et al. 1986; PLENGE et al. 2000).

¹*Corresponding author:* Institute for Genome Sciences and Policy, Duke University, Box 3382, 101 Science Dr., Durham, NC 27708.
E-mail: hunt.willard@duke.edu

In earlier studies, the *Xce* locus was mapped to a region between the ectodysplasin-A (*Eda*, at position 94.5 Mb in Mm Build 34) and the phosphoglycerate kinase (*Pgk1*, 100.7 Mb) genes, a region that encompasses the *X inactivation center* (*Xic*) (CATTANACH *et al.* 1970, 1982; CATTANACH and PAPWORTH 1981). The *Xist* locus, which encodes a noncoding RNA required *in cis* to initiate X inactivation, is located in the *Xic* (BORSANI *et al.* 1991; BROCKDORFF *et al.* 1991; LEE *et al.* 1999), along with its antisense counterpart *Tsix* (LEE *et al.* 1999). However, an ancestral recombination event identified in the well-characterized strain JU/Ct excluded these as positional candidates for *Xce* (SIMMLER *et al.* 1993). Although this analysis suggested that the distal boundary of the *Xce* candidate region was located between *DXPas29* and *DXPas28* (98 and 97.9 Mb, respectively), the proximal boundary of the candidate interval has not yet been refined.

Although the nature of the *Xce* locus and its molecular mode of action has not yet been identified, most models of X inactivation (LYON 1971; BROWN and CHANDRA 1973; RUSSELL and CACHEIRO 1978; RASTAN 1983) hypothesize that it serves as a binding site for *trans*-acting factors that in turn regulate the expression of other loci in the *Xic*, such as *Xist* or *Tsix*. The various *Xce* alleles are thus predicted to have differential binding affinities for this factor (or factors), leading to a bias in the choice between chromosomes. While no such factors have been identified to date, mutagenesis has uncovered three candidate loci, all of which are autosomally encoded (*Xiaf1–3*) (PERCEC *et al.* 2002, 2003). We have shown previously that naturally occurring genetic variation between inbred mouse strains can also influence X chromosome choice (CHADWICK and WILLARD 2005), suggesting that it may be possible to identify additional modifiers of choice in inbred strains using standard quantitative trait (QTL) mapping approaches.

As the precise location and nature of the *Xce* locus is not known, genetic studies of X inactivation in mice rely upon tightly linked markers to infer *Xce* genotype. Previously, the markers *DXMit18* and *DXMit171* were used for this purpose (PERCEC *et al.* 2002, 2003). However, we found that progeny testing did not always support this interval (data not shown), suggesting that *Xce* in fact may lie proximal to these markers. In this study, we used QTL mapping techniques to define the *Xce* candidate interval to a maximum 1.85-Mb region of the mouse X chromosome and provide progeny test data to support this localization. We then used a similar approach to search for additional naturally occurring modifiers of X inactivation patterns.

MATERIALS AND METHODS

Mice and mouse crosses: C57BL/6J (B6), BALB/cByJ (BALB), and CAST/Ei (CAST) mice used in these crosses were purchased from The Jackson Laboratory. Mice were housed in accordance with Institutional Animal Use and Care Committee guidelines. F_1 crosses were carried out using B6 or BALB females and CAST males. F_1 progeny were then intercrossed to generate F_2 females. In addition, we backcrossed B6CASTF$_1$ females to B6 males or BALBCASTF$_1$ females to BALB males for two to eight generations, selecting for the presence of CAST X chromosome alleles at each backcross generation. After the first backcross generation, both males and females were used for backcrossing. Ear biopsies were collected at weaning for later RNA isolation.

RNA isolation and cDNA synthesis: RNA was isolated from ear biopsies and whole-mouse embryos using the RNeasy miniprep kit (QIAGEN, Chatsworth, CA), according to the manufacturer's recommendations. For ear RNA, the modified fibrous tissue protocol was used. cDNA synthesis was carried out as described (PERCEC *et al.* 2003), using random primers.

Allele-specific expression assays: The *Pctk1* expression assay was carried out as described previously (PLENGE *et al.* 2000), except that products were separated and analyzed on an ABI 3100 capillary sequencer. We designed an assay similar to *Idh3g* for use with animals that were not informative at *Pctk1*. This *Idh3g* assay was performed as the *Pctk1* assay with the following differences: the primers used were 5'-AACTATGGCCATGTG TATGC-3' and 5'-CTCCAATATCTGGGGTATGC-3', and the products were digested with *Taq*αI.

Genotyping: All genotyping was carried out by PCR amplification of microsatellite markers, and PCR products were separated on an ABI 3100 capillary sequencer. Genetic location of markers and primer sequences were taken from the Mouse Genome Database (BLAKE *et al.* 2003).

Embryo dissections: Embryos were collected at 10.5 days post-coitum (dpc) according to established protocols (HOGAN *et al.* 1994). Mating was ascertained by checking for vaginal plugs, with the first day after mating designated as 0.5 dpc. The sex of embryos was determined by PCR amplification of the *Smcx* and *Smcy* genes, as described previously (MROZ *et al.* 1999).

QTL mapping: QTL mapping was performed by standard interval mapping (LANDER and BOTSTEIN 1989), using the software R/qtl (BROMAN *et al.* 2003), an add-on package to the general statistical software, R (IHAKA and GENTLEMAN 1996). Statistical significance with adjustment for a genomewide scan was determined by a permutation test (CHURCHILL and DOERGE 1994); 1000 permutation replicates were used.

SNP discovery: To identify SNPs that differentiated the CAST haplotype from BALB and B6 haplotypes, genomic DNA from each strain was PCR amplified and sequenced using the BigDye Terminator v 3.1 cycle sequencing kit (Applied Biosystems, Foster City, CA). Polymorphic sites were identified by directly comparing sequences from the three strains. Sequenced regions, primers used, and SNP genotypes are listed in Table 1.

RESULTS

Identification of major genetic influences on X inactivation patterns: We have demonstrated previously that genetic background differences segregating in the B6CASTF$_2$ cross resulted in significant effects on early events that determine the X inactivation pattern (the proportion of cells that have one or the other chromosome active) in *Xce* heterozygous mice (CHADWICK and WILLARD 2005). X inactivation can be considered a quantitative trait, where the X inactivation pattern is treated as a continuous quantitative phenotype. To determine
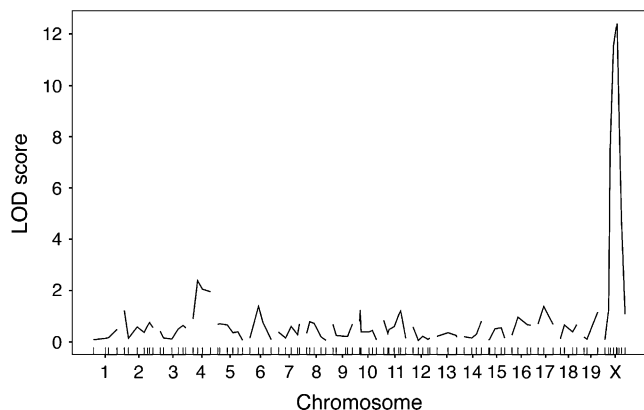
FIGURE 1.—LOD curves from the B6CASTF$_2$ *Xce* heterozygotes/*Xce* homozygotes whole-genome scan. LOD score is on the *y*-axis; chromosomes are on the *x*-axis. Genetic location of markers tested are indicated by tick marks on the *x*-axis. The genomewide level of significance as determined by permutation tests is LOD = 3.5. Significance was reached only on the X chromosome, indicating that *Xce* is the only major locus influencing X inactivation patterns in this cross.

FIGURE 2.—X chromosome LOD curve from extended *Xce* heterozygote/*Xce* homozygote analysis (*n* = 655, from B6CAST and BALBCAST intercrosses and backcrosses). LOD scores are on the *y*-axis; genetic positions of markers tested (from MGD) are on the *x*-axis. The genetic locations of *Pctk1*, *Idh3g*, *Xist*/*Tsix*/*Xite*, *DXMit41*, and *DXMit171* are indicated. The 1.5-LOD confidence interval is indicated by a short, solid horizontal line, intersected by a vertical line indicating the peak. This suggests that the *Xce* locus is located between *DXMit41* and *DXMit171*.

whether these effects represented a global influence on X chromosome choice (regardless of *Xce* genotype), we used a QTL mapping strategy in a population of B6CASTF$_2$ *Xce* homozygotes and *Xce* heterozygotes. We genotyped 72 B6CASTF$_2$ *Xce* heterozygous and 28 B6CASTF$_2$ *Xce* homozygous females using a panel of microsatellite markers with ~20 cM average spacing based on one developed previously (IAKOUBOVA *et al.* 2000). We identified a single major QTL (Figure 1) in this cross. As this locus was X linked, it seemed likely that this association was due to *Xce*. Thus, we conclude that *Xce* is the major locus in the genome that influences X chromosome choice.

Defining the *Xce* candidate region: Although the *Xce* locus was first described nearly 40 years ago (CATTANACH and ISAACSON 1967), its genomic localization on the X chromosome has not been rigorously defined and encompasses a large genetic interval (CATTANACH *et al.* 1970, 1982; CATTANACH and PAPWORTH 1981; SIMMLER *et al.* 1993). We sought to use QTL approaches in an effort to further define the *Xce* candidate interval.

For this analysis, we used a sample of B6CAST (*n* = 528) and BALBCAST (*n* = 127) female mice collected from a variety of crosses (intercrosses and backcrosses) that had previously been bred for other purposes. This sample was not predicated on the *Xce* genotype, and analysis included mice both heterozygous (*Xce^b*/*Xce^e* or *Xce^a*/*Xce^e*) and homozygous (*Xce^b*/*Xce^b* or *Xce^a*/*Xce^a*) at *Xce*. However, each sample was heterozygous for at least one of the marker genes used to determine the X inactivation pattern, *Pctk1* (5.5 cM) or *Idh3g* (29.5 cM). For each individual, we determined the X inactivation pattern and the X chromosome genotypes for markers spanning the X chromosome (*DXMit55*: 1.4 cM; *DXMit165*: 14 cM; *DXMit75*: 18.9 cM; *DXMit42*: 30.6 cM;
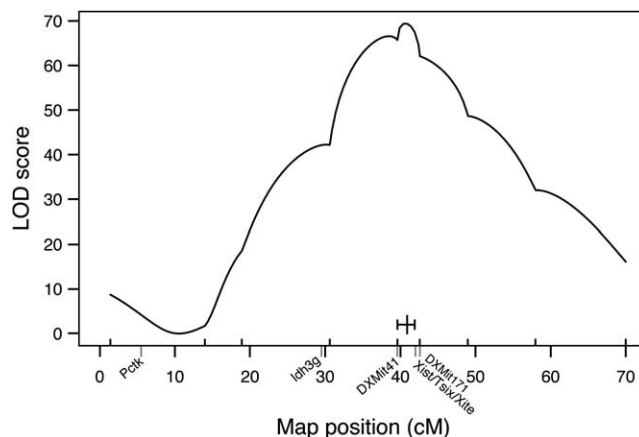
DXMit41: 39.6 cM; *DXMit97*: 49 cM; *DXMit151*: 58 cM; and *DXMit156*: 70 cM), including one marker thought to be tightly linked to the *Xce* locus (*DXMit171*: 42.6 cM). Interval mapping with this data set (Figure 2) indicated that the *Xce* locus was located within a 2.3-cM region (1.5-LOD confidence interval) spanning from 39.6 cM (*DXMit41*) to 41.9 cM (slightly proximal of *DXMit171*), consistent with and refining previous mapping studies (CATTANACH *et al.* 1970, 1982; CATTANACH and PAPWORTH 1981; SIMMLER *et al.* 1993).

To refine further the candidate region, we identified nine animals (six from B6CAST crosses, three from BALBCAST crosses) with crossovers between *DXMit41* and *DXMit171* and genotyped them at intervening markers: *DXMit168*, *DXMit115*, *DXPas28*, *DXPas29*, and *DXPas31* (used by SIMMLER *et al.* 1993). The haplotypes and X inactivation patterns for these individuals are shown in Figure 3. It is important to note that the apparent nonrandom representation of alleles in these females (all carrying the CAST allele at *DXMit41* while carrying B6 or BALB alleles at *DXMit171*) reflects the requirement of our approach: the recombinant chromosomes also need to carry CAST alleles at either *Pctk* or *Idh3g* (both located proximal to this region) such that X inactivation assays can be carried out in female progeny. To classify these animals into phenotypic classes (*Xce* homozygous like and *Xce* heterozygous like), we determined the probability that each individual's X inactivation pattern fell into a normal distribution with a mean of 0.5 and SD of 0.1 (predicted for *Xce* homozygotes given a random choice; PLENGE *et al.* 2000) or with a mean of 0.29 and SD of 0.13 (CHADWICK and WILLARD 2005). As a result of this analysis, we identified
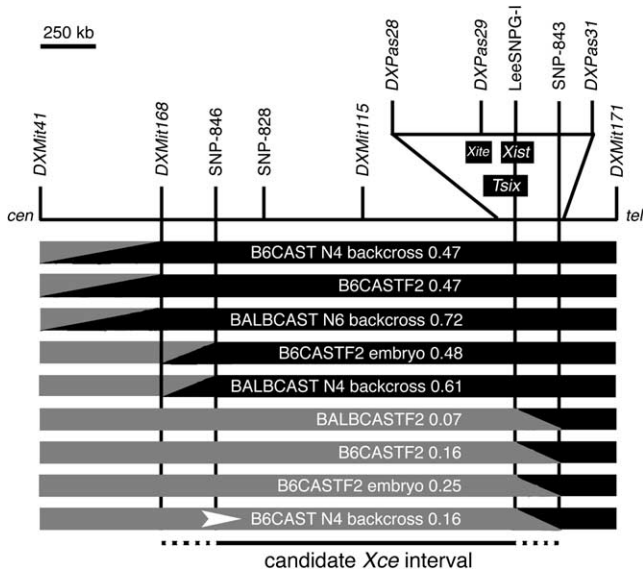
Figure 3.—Haplotype map of females with crossovers between *DXMit41* and *DXMit171*. Heterozygous genotypes (B6/CAST or BALB/CAST) are indicated as shaded segments; homozygous genotypes (B6/B6 or BALB/BALB) are indicated as solid segments. Diagonal regions between markers indicate the location of crossover events. The locations of *Xite*, *Tsix*, and *Xist* are indicated. The genetic background and X inactivation pattern of each individual are also indicated. Animals with homozygous genotypes between SNP-846 and *DXMit171* had *Xce* homozygous-like X inactivation patterns, suggesting that the proximal boundary of the *Xce* interval lay between *DXMit168* and SNP-846. Conversely, animals with heterozygous genotypes between *DXMit41* and SNP-843 had *Xce* heterozygous-like X inactivation patterns, suggesting that the distal boundary of the candidate interval lay between LeeSNPG-I and SNP-843. The B6CAST N4 backcross individual selected for further progeny testing (Figure 4) is indicated by an arrowhead.

five individuals predicted to be *Xce* homozygotes (X inactivation patterns 0.47–0.72, 76–96% probability of being homozygous at *Xce*) and four mice predicted to be *Xce* heterozygotes (X inactivation patterns 0.07–0.25, 94–99% probability of being heterozygous at *Xce*). Three of the so-defined *Xce* homozygous females had heterozygous genotypes at *DXMit168* but homozygous genotypes at *DXMit115*, thus defining the proximal boundary of the candidate interval. In addition, we also identified four *Xce* heterozygous females that had heterozygous genotypes at *DXPas29* but homozygous genotypes at *DXPas31*, indicating that the distal boundary of the candidate interval lay between these two markers. As no other published microsatellite markers were available, we sequenced selected genomic segments in the relevant strains and identified additional SNPs in these regions (between *DXMit168* and *DXMit115* and between *DXPas29* and *DXPas31*) that distinguished the CAST haplotype from that of the two classical inbred strains used in our crosses (Table 1). Both individuals with recombinant haplotypes between *DXMit168* and *DXMit115* had crossover events close to *DXMit168*; while

TABLE 1

SNPs identified and tested in this study

SNP	Primer A	Primer B	No. of SNPs in amplicon	B6/BALB allele	CAST allele
SNP-846	5'-GGCTAAGCCATCACTTATCC-3'	5'-AAGATTCCTAACTGTTCTGGG-3'	3 (all in dbSNP)	GCT	TTC
SNP-828	5'-CCATGGAGATGATGACAAGC-3'	5'-GGCCTACAAAGCGACTTCC-3'	1 novel	A	G
LeeSNPG-I[a]	5'-GCTTGGTTCGTCTATCTTGTGGG-3'	5'-CCAGAGTCTGATGTAACGGAGG-3'	1	Not digested by *ScrFI*	Digested by *ScrFI*
SNP-843	5'-TGTTTCCATGCCTCAGAAGC-3'	5'-GAACCACACTGCTTAACTAGC-3'	3 novel 2 in dbSNP	TACCA	ACTAG

SNPs were genotyped by PCR amplification of genomic DNA using the primers indicated followed by sequencing.

[a] This assay was published in Stavropoulos *et al.* (2001). To genotype this SNP, genomic DNA was PCR amplified with the primers indicated and digested with *ScrFI*, and products were separated by gel electrophoresis.
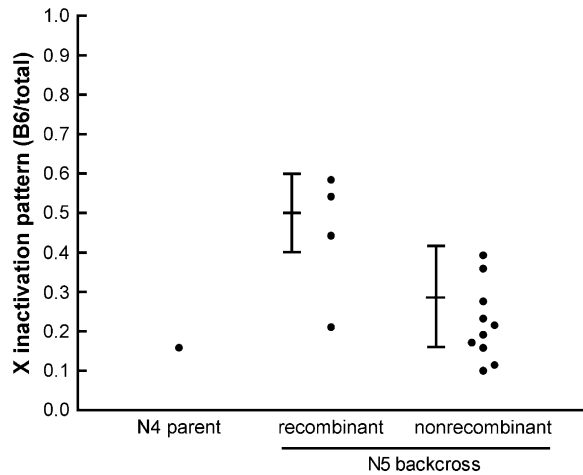
FIGURE 4.—Progeny testing to confirm the distal boundary of the *Xce* candidate region. A B6CAST N4 backcross female with a crossover between LeeSNPG-I and SNP-843 was crossed to a B6 male and the X inactivation patterns of the N5 progeny were determined. The predicted range of X inactivation patterns for *Xce* homozygotes (mean = 0.5, SD = 0.1, as suggested by PLENGE *et al.* 2000) and *Xce* heterozygotes arising from this cross (mean = 0.29, SD = 0.13, from CHADWICK and WILLARD 2005) are indicated. "Recombinant" animals do not carry the heterozygous haplotype of the parent in the *DXMit41–DXMit171* candidate region; "nonrecombinant" animals have the same haplotype as the N4 parent. As expected, N5 females with the recombinant haplotype have X inactivation patterns that are generally consistent with an *Xce* homozygous genotype, while N5 females with the nonrecombinant haplotype have X inactivation patterns consistent with an *Xce* heterozygous genotype.

they had heterozygous genotypes at *DXMit168*, both had B6 genotypes at SNP-846. All four individuals with recombinant haplotypes between *DXPas29* and *DXPas31* had crossover events that occurred within a 165-kb region between LeeSNPG-I (a SNP located within the *Xist* locus; STAVROPOULOS *et al.* 2001) and SNP-843. Thus, by analyzing recombinant chromosomes, we have established that the *Xce* candidate interval spans a minimum of 1.5 Mb and a maximum of 1.85 Mb from *DXMit168* (96.3 Mb) to SNP-843 (98.1 Mb), as shown in Figure 3.

To confirm these results, we progeny tested a B6CAST N4 backcross female that had a recombinant haplotype between LeeSNPG-I and SNP-843 (Figure 4; the individual tested is indicated in Figure 3). The X inactivation patterns of the N5 backcross progeny confirmed our placement of the distal boundary of the *Xce* candidate region; female progeny that had inherited the CAST haplotype (and thus that were heterozygous throughout the *Xce* candidate region) had skewed, *Xce* heterozygous-like X inactivation patterns, while progeny that had inherited the B6 haplotype in this region generally had X inactivation patterns in the *Xce* homozygous-like range. This confirmed our placement of the distal *Xce* boundary between LeeSNPG-I and SNP-843.

Nonrandom distribution of crossovers in the *DXMit41–DXMit171* interval: While identifying recombination breakpoints in the nine females that were recombinant between *DXMit41* and *DXMit171*, we observed a nonrandom distribution of crossovers in these individuals. Although we found two independent crossover events occurring in the 258-kb region between *DXMit168* and SNP-846 and four independent crossover events in the 165-kb region between LeeSNPG-I and SNP-843, we did not observe a single crossover in the intervening ~1.5 Mb (Figure 3). To determine whether this apparent suppression of recombination was unusual for an area of this physical size, we sought to calculate the relationship between genetic and physical distances in the *DXMit41–DXMit171* interval, compared to another region of the X chromosome.

We collected genotype information from individuals, both male and female, arising from B6CAST crosses in which the mother carried a fully nonrecombinant CAST X chromosome opposite a nonrecombinant B6 X chromosome. This situation was true in both intercrosses ($n = 921$) and in some backcrosses ($n = 612$). We selected individuals for which we had genotype information at both *DXMit41* (39.6 cM) and *DXMit171* (42.6 cM) ($n = 967$), and individuals with genotype information at both *DXMit165* (14 cM) and *DXMit75* (18.9 cM) ($n = 1297$). We observed 11 crossovers between *DXMit41* and *DXMit171* in 967 individuals, a genetic distance of 1.1 cM. The actual physical distance between the two was 2.74 Mb, and the calculated recombination rate was thus 0.40 cM/Mb in this interval. In the *DXMit165–DXMit75* interval, we observed 93 crossovers in 1297 meioses, a genetic distance of 7 cM over a 17.8-Mb region, or 0.39 cM/Mb, which is similar to that observed in the *DXMit41–DXMit171* interval and to the genomewide average (0.5 cM/Mb) (BUCHNER *et al.* 2003; KELMENSON *et al.* 2005). If recombination rates were consistent across the entire length of the chromosome, we would have expected to identify three or four individuals with crossovers between SNP-846 and LeeSNPG-I. Conversely, the 165-kb segment between LeeSNPG-I and SNP-843 appears to contain a recombination hotspot with a recombination frequency of 3.6 cM/Mb, more than sevenfold higher than the genome average.

QTL mapping to identify autosomal modifiers of *Xce*: Because QTL mapping approaches proved quite useful in refining the *Xce* candidate region, we used a similar strategy to search for additional loci that influenced X inactivation patterns (Figure 5). To control for the effect of the major X-linked QTL (*i.e.*, *Xce*), we used only *Xce* heterozygous females, who would be predicted to have a similar range of X inactivation patterns. We genotyped 72 *Xce* heterozygous B6CASTF$_2$ females at loci across the genome (20 cM average spacing) with the panel of microsatellite markers used previously. Interval mapping identified one region on chromosome 4 that showed suggestive association with differences in the
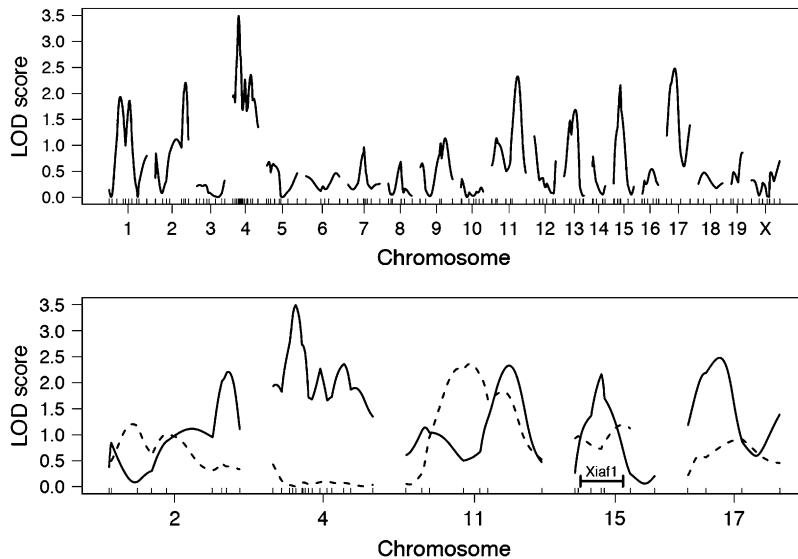
FIGURE 5.—LOD curves from B6CASTF$_2$ *Xce* heterozygote whole-genome scan. (Top) The LOD scores from the whole-genome analysis of B6CASTF$_2$ *Xce* heterozygous adult samples. The genomewide significance level as determined by permutation tests is LOD = 3.5. (Bottom) The LOD scores of adults (solid lines) and embryos (dashed lines) for the five most significant chromosomes from the adult analysis. The location of *Xiaf1* on chromosome 15 is indicated (PERCEC *et al.* 2002).

X inactivation pattern, although this fell slightly below the genomewide level of significance determined by permutation testing (LOD = 3.49, $P = 0.08$). We added additional markers in this region, but this did not increase the level of significance.

To confirm or exclude this region as a candidate locus, we sought to reduce variation in the phenotype by using whole-embryo RNA rather than RNA obtained from adult ear biopsies (CHADWICK and WILLARD 2005), in principle making it easier to detect potential QTL. Thus, we genotyped *Xce^b*/*Xce^c* B6CASTF$_2$ embryos ($n = 79$) on the chromosomes with the highest LOD scores in the initial scan: chromosomes 2, 4, 11, 15, and 17. None of these chromosomes showed a significant association with the phenotype in whole embryos, including chromosome 4, which was most significant in the initial screen (Figure 5), and chromosome 15, which harbors *Xiaf1*, an ENU-induced mutation known to influence X chromosome choice (PERCEC *et al.* 2002, 2003). Thus, while we have demonstrated that genetic background plays a role in influencing X inactivation patterns (CHADWICK and WILLARD 2005), we were not able to identify any significantly associated autosomal loci with the available data.

DISCUSSION

A genetically defined candidate region for *Xce*: In this study we have used a combination of QTL mapping, analysis of recombinant chromosomes, and progeny testing to demonstrate conclusively that *Xce* is the only major locus that influences X inactivation patterns (and likely, therefore, X chromosome choice) in the mouse crosses analyzed. Furthermore, we defined a 1.85-Mb region of the mouse X chromosome that contains most (if not all) elements of the *Xce* locus, as this interval accounts fully for the known effects of *Xce* on X inactivation patterns. As the nature of and the underlying

molecular mechanisms of *Xce* remain elusive, this has implications for future study of X chromosome choice.

Previously, SIMMLER *et al.* (1993) attempted to map the *Xce* locus by examining microsatellite marker haplotypes of mouse strains with well-characterized *Xce* alleles. They observed discordant alleles at *DXPas29* and *DXPas31* in the JU/Ct strain relative to other *Xce^b* strains, indicating that the *Xce* locus lay proximal to *DXPas29* and thus was distinct from *Xist*. Combined with the results of our study, the *Xce* candidate interval could be even smaller than the region identified here. However, a potential limitation of the Simmler *et al.* study is its reliance upon microsatellite repeat polymorphisms, which are known to have somewhat higher mutation rates than other sequences (HASTBACKA *et al.* 1992). Thus, in the absence of additional recombinants, we feel it is prudent to consider the larger interval as a guide to further study. Our data establish a relatively similar distal boundary for the *Xce* candidate interval (on the basis of genetic mapping and progeny testing), but do not allow us to exclude *Xist*, *Tsix*, or *Xite* as *Xce* candidate loci. This allows for the possibility that polymorphisms located either within these transcripts or in their regulatory regions may contribute to the bias in X chromosome choice observed in *Xce* heterozygous females. In fact, in humans a rare variant found within the *XIST* promoter has been shown to cause significant skewing of the X inactivation pattern (PLENGE *et al.* 1997). This bias in determining the X inactivation pattern is thought to be the result of a dramatic increase in CTCF binding to the XIST promoter on the variant allele (PUGACHEVA *et al.* 2005).

In addition to clarifying the relationship between *Xce* candidate sequences and known genes within the *Xic*, we have defined ~1.7 Mb of additional candidate sequence that can now be tested. Although it is tempting to postulate that all X chromosome choice elements are located in the immediate vicinity of *Xist*

and *Tsix*, it will be important to consider the remainder of the candidate interval. Subsequent studies may further define critical sequences by identifying additional recombinants, by establishing congenic lines carrying overlapping introgressed segments, or by using a sequence substitution approach in female embryonic stem cells.

It is interesting to note the nonrandom distribution of crossover events that we observed within the *Xce* candidate region. While we observed no recombination in the 1.5-Mb region between SNP-846 and LeeSNPG-I, recombination in the adjacent region (LeeSNPG-I–SNP-843) appeared to be over sevenfold higher than the genomewide average (Buchner *et al.* 2003; Kelmenson *et al.* 2005). Several recombination hotspots have been defined in mammals, the most well characterized being at the major histocompatibility complexes of humans and mice (Shiroishi *et al.* 1990; Jeffreys *et al.* 2001). In yeast, recombination hotspots are relatively common and distributed throughout the genome (Gerton *et al.* 2000); recent evidence suggests that this may also be true in mammalian genomes (Crawford *et al.* 2004; McVean *et al.* 2004). If this is indeed the case, the "granular" distribution of crossovers that we observed in the *Xce* region may not be unusual. Alternatively, the *Xce* locus may be marked by genomic rearrangements (such as inversions) between strains, as these have been shown to bias recombination rates (Singleton 1964), even in mice (Zheng *et al.* 1999; Klysik *et al.* 2004). Such genomic differences could either ablate binding sites for *trans*-acting factors entirely or bring these sites closer to (or farther from) other enhancer elements or the *Tsix* promoter. Future genomic studies in strains with well-characterized *Xce* alleles may address this question.

An approach for identifying *trans*-acting factors influencing X chromosome choice: Using QTL mapping techniques, we were able to define the *Xce* candidate interval on the mouse X chromosome. However, we were unable to identify autosomal modifier loci using a similar strategy in our initial data set of 72 *Xce* heterozygous F_2 females. Nonetheless, we believe that this approach may have great potential for identifying *trans*-acting factors, although a significantly larger sample size would likely be required. Another possibility is to investigate other crosses, particularly with additional wild-derived strains. Wild-derived inbred strains are highly polymorphic relative to classical inbred strains, and many such polymorphisms could have functional consequences (Ideraabdullah *et al.* 2004) that would obviate the need for extensive mutagenesis screens.

Although our initial screen did identify one suggestive autosomal QTL, we were unable to confirm this locus in F_2 embryos. We can imagine several scenarios that could explain this. First, as is true in any linkage mapping experiment, the initial identification of a locus on chromosome 4 could have been a false positive. Alternatively, the QTL could exert a subtle effect that we were able to identify in the initial experiment, and for

which we had low power to detect in the second, smaller experiment. A further possibility is that the chromosome 4 QTL affected an aspect of X inactivation, such as clone size, that would be irrelevant or undetectable in whole embryos. A QTL that affected clone size, perhaps by altering the timing of X inactivation, would not be detectable in embryos, where we determined X inactivation patterns in whole animals. Aside from this limitation, whole embryos would appear to be a promising system with which to further investigate the genetic regulation of X inactivation. The significant reduction in phenotypic variation relative to adult populations makes them well suited both for QTL analyses and for further study of X inactivation choice in general.

LITERATURE CITED

Blake, J. A., J. E. Richardson, C. J. Bult, J. A. Kadin and J. T. Eppig, 2003 MGD: the Mouse Genome Database. Nucleic Acids Res. **31:** 193–195.

Borsani, G., R. Tonlorenzi, M. C. Simmler, L. Dandolo, D. Arnaud *et al.*, 1991 Characterization of a murine gene expressed from the inactive X chromosome. Nature **351:** 325–329.

Brockdorff, N., A. Ashworth, G. F. Kay, P. Cooper, S. Smith *et al.*, 1991 Conservation of position and exclusive expression of mouse Xist from the inactive X chromosome. Nature **351:** 329–331.

Broman, K. W., H. Wu, S. Sen and G. A. Churchill, 2003 R/qtl: QTL mapping in experimental crosses. Bioinformatics **19:** 889–890.

Brown, S. W., and H. S. Chandra, 1973 Inactivation system of the mammalian X chromosome. Proc. Natl. Acad. Sci. USA **70:** 195–199.

Buchner, D. A., M. Trudeau, A. L. George, Jr., L. K. Sprunger and M. H. Meisler, 2003 High-resolution mapping of the sodium channel modifier Scnm1 on mouse chromosome 3 and identification of a 1.3-kb recombination hot spot. Genomics **82:** 452–459.

Cattanach, B. M., and J. H. Isaacson, 1967 Controlling elements in the mouse X chromosome. Genetics **57:** 331–346.

Cattanach, B. M., and D. Papworth, 1981 Controlling elements in the mouse. V. Linkage tests with X-linked genes. Genet. Res. **38:** 57–70.

Cattanach, B. M., and C. E. Williams, 1972 Evidence of non-random X chromosome activity in the mouse. Genet. Res. **19:** 229–240.

Cattanach, B. M., C. E. Pollard and J. N. Perez, 1969 Controlling elements in the mouse X-chromosome. I. Interaction with the X-linked genes. Genet. Res. **14:** 223–235.

Cattanach, B. M., J. N. Perez and C. E. Pollard, 1970 Controlling elements in the mouse X-chromosome. II. Location in the linkage map. Genet. Res. **15:** 183–195.

Cattanach, B. M., T. H. Bucher and S. J. Andrews, 1982 Location of *Xce* in the mouse X chromosome and effects on PGK-1 expression. Genet. Res. **40:** 103–104.

Chadwick, L. H., and H. F. Willard, 2005 Genetic and parent-of-origin influences on X chromosome choice in Xce heterozygous mice. Mamm. Genome **16:** 691–699.

Churchill, G. A., and R. W. Doerge, 1994 Empirical threshold values for quantitative trait mapping. Genetics **138:** 963–971.

Crawford, D. C., T. Bhangale, N. Li, G. Hellenthal, M. J. Rieder *et al.*, 2004 Evidence for substantial fine-scale variation in recombination rates across the human genome. Nat. Genet. **36:** 700–706.

de La Casa-Esperon, E., J. C. Loredo-Osti, F. Pardo-Manuel de Villena, T. L. Briscoe, J. M. Malette *et al.*, 2002 X chromosome

effect on maternal recombination and meiotic drive in the mouse. Genetics **161:** 1651–1659.

Drews, U., S. R. Blecher, D. A. Owen and S. Ohno, 1974 Genetically directed preferential X-activation seen in mice. Cell **1:** 4–8.

Gerton, J. L., J. DeRisi, R. Shroff, M. Lichten, P. O. Brown *et al.*, 2000 Inaugural article: global mapping of meiotic recombination hotspots and coldspots in the yeast Saccharomyces cerevisiae. Proc. Natl. Acad. Sci. USA **97:** 11383–11390.

Hastbacka, J., A. de la Chapelle, I. Kaitila, P. Sistonen, A. Weaver *et al.*, 1992 Linkage disequilibrium mapping in isolated founder populations: diastrophic dysplasia in Finland. Nat. Genet. **2:** 204–211.

Hogan, B., R. Beddington, F. Costantini and E. Lacey, 1994 *Manipulating the Mouse Embryo: A Laboratory Manual.* Cold Spring Harbor Laboratory Press, Cold Spring Harbor, NY.

Huynh, K. D., and J. T. Lee, 2001 Imprinted X inactivation in eutherians: a model of gametic execution and zygotic relaxation. Curr. Opin. Cell Biol. **13:** 690–697.

Iakoubova, O. A., C. L. Olsson, K. M. Dains, J. Choi, I. Kalcheva *et al.*, 2000 Microsatellite marker panels for use in high-throughput genotyping of mouse crosses. Physiol. Genomics **3:** 145–148.

Ideraabdullah, F. Y., E. de la Casa-Esperon, T. A. Bell, D. A. Detwiler, T. Magnuson *et al.*, 2004 Genetic and haplotype diversity among wild-derived mouse inbred strains. Genome Res. **14:** 1880–1887.

Ihaka, R., and R. Gentleman, 1996 R: a language for data analysis and graphics. J. Comput. Graph. Stat. **5:** 299–314.

Jeffreys, A. J., L. Kauppi and R. Neumann, 2001 Intensely punctate meiotic recombination in the class II region of the major histocompatibility complex. Nat. Genet. **29:** 217–222.

Johnston, P. G., and B. M. Cattanach, 1981 Controlling elements in the mouse. IV. Evidence of non-random X-inactivation. Genet. Res. **37:** 151–160.

Kelmenson, P. M., P. Petkov, X. Wang, D. C. Higgins, B. J. Paigen *et al.*, 2005 A torrid zone on mouse chromosome 1 containing a cluster of recombinational hotspots. Genetics **169:** 833–841.

Klysik, J., C. Dinh and A. Bradley, 2004 Two new mouse chromosome 11 balancers. Genomics **83:** 303–310.

Krietsch, W. K., M. Fehlau, P. Renner, T. Bucher and R. Fundele, 1986 Expression of X-linked phosphoglycerate kinase in early mouse embryos homozygous at the Xce locus. Differentiation **31:** 50–54.

Lander, E. S., and D. Botstein, 1989 Mapping Mendelian factors underlying quantitative traits using RFLP linkage maps. Genetics **121:** 185–199.

Lee, J. T., L. S. Davidow and D. Warshawsky, 1999 Tsix, a gene antisense to Xist at the X-inactivation centre. Nat. Genet. **21:** 400–404.

Lyon, M. F., 1961 Gene action in the X-chromosome of the mouse (*Mus musculus* L.). Nature **190:** 372–373.

Lyon, M. F., 1971 Possible mechanisms of X chromosome inactivation. Nat. New Biol. **232:** 229–232.

McVean, G. A., S. R. Myers, S. Hunt, P. Deloukas, D. R. Bentley *et al.*, 2004 The fine-scale structure of recombination rate variation in the human genome. Science **304:** 581–584.

Mroz, K., L. Carrel and P. A. Hunt, 1999 Germ cell development in the XXY mouse: evidence that X chromosome reactivation is independent of sexual differentiation. Dev. Biol. **207:** 229–238.

Perceg, I., R. M. Plenge, J. H. Nadeau, M. S. Bartolomei and H. F. Willard, 2002 Autosomal dominant mutations affecting X inactivation choice in the mouse. Science **296:** 1136–1139.

Perceg, I., J. L. Thorvaldsen, R. M. Plenge, C. J. Krapp, J. H. Nadeau *et al.*, 2003 An *N*-ethyl-*N*-nitrosourea mutagenesis screen for epigenetic mutations in the mouse. Genetics **164:** 1481–1494.

Plenge, R. M., B. D. Hendrich, C. Schwartz, J. F. Arena, A. Naumova *et al.*, 1997 A promoter mutation in the XIST gene in two unrelated families with skewed X-chromosome inactivation. Nat. Genet. **17:** 353–356.

Plenge, R. M., I. Perceg, J. H. Nadeau and H. F. Willard, 2000 Expression-based assay of an X-linked gene to examine effects of the X-controlling element (Xce) locus. Mamm. Genome **11:** 405–408.

Pugacheva, E. M., V. K. Tiwari, Z. Abdullaev, A. A. Vostrov, P. T. Flanagan *et al.*, 2005 Familial cases of point mutations in the XIST promoter reveal a correlation between CTCF binding and pre-emptive choices of X chromosome inactivation. Hum. Mol. Genet. **14:** 953–965.

Rastan, S., 1982 Primary non-random X-inactivation caused by controlling elements in the mouse demonstrated at the cellular level. Genet. Res. **40:** 139–147.

Rastan, S., 1983 Non-random X-chromosome inactivation in mouse X-autosome translocation embryos: location of the inactivation centre. J. Embryol. Exp. Morphol. **78:** 1–22.

Russell, L. B., and N. L. Cacheiro, 1978 The use of mouse X-autosome translocations in the study of X-inactivation pathways and nonrandomness. Basic Life Sci. **12:** 393–416.

Sado, T., and A. C. Ferguson-Smith, 2005 Imprinted X inactivation and reprogramming in the preimplantation mouse embryo. Hum. Mol. Genet. **14**(Suppl. 1): R59–R64.

Sado, T., Z. Wang, H. Sasaki and E. Li, 2001 Regulation of imprinted X-chromosome inactivation in mice by Tsix. Development **128:** 1275–1286.

Shiroishi, T., N. Hanzawa, T. Sagai, M. Ishiura, T. Gojobori *et al.*, 1990 Recombinational hotspot specific to female meiosis in the mouse major histocompatibility complex. Immunogenetics **31:** 79–88.

Simmler, M. C., B. M. Cattanach, C. Rasberry, C. Rougeulle and P. Avner, 1993 Mapping the murine Xce locus with (CA)n repeats. Mamm. Genome **4:** 523–530.

Singleton, J. R., 1964 A mechanism intrinsic to heterozygous inversions affecting observed recombination frequencies in adjacent regions. Genetics **49:** 541–560.

Stavropoulos, N., N. Lu and J. T. Lee, 2001 A functional role for Tsix transcription in blocking Xist RNA accumulation but not in X-chromosome choice. Proc. Natl. Acad. Sci. USA **98:** 10232–10237.

Takagi, N., and M. Sasaki, 1975 Preferential inactivation of the paternally derived X chromosome in the extraembryonic membranes of the mouse. Nature **256:** 640–642.

Wang, J., J. Mager, Y. Chen, E. Schneider, J. C. Cross *et al.*, 2001 Imprinted X inactivation maintained by a mouse Polycomb group gene. Nat. Genet. **28:** 371–375.

West, J. D., and V. M. Chapman, 1978 Variation for X chromosome expression in mice detected by electrophoresis of phosphoglycerate kinase. Genet. Res. **32:** 91–102.

Zheng, B., M. Sage, W. W. Cai, D. M. Thompson, B. C. Tavsanli *et al.*, 1999 Engineering a mouse balancer chromosome. Nat. Genet. **22:** 375–378.